A new approach to vented deflagration modeling

Tolias, I.C.[1], Venetsanos, A.G.[1]
[1] Environmental Research Laboratory, National Center for Scientific Research Demokritos, Agia Paraskevi, 15310, Greece, tolias@ipta.demokritos.gr

ABSTRACT

In the present work, CFD simulations of a hydrogen deflagration experiment are performed. The experiment, carried out by KIT, was conducted in a 1 m^3 enclosure with a square vent of 0.5 m^2 located in the center of one of its walls. The enclosure was filled with homogeneous hydrogen-air mixture of 18% v/v before ignition at its back-wall. As the flame propagates away from the ignition point, unburned mixture is forced out through the vent. This mixture is ignited when the flame passes through the vent, initiating a violent external explosion which leads to a rapid increase in pressure. The work focuses on the modeling of the external explosion phenomenon. A new approach is proposed in order to predict with accuracy the strength of external explosions using Large Eddy Simulation. The new approach introduces new relations to account for the interaction between the turbulence and the flame front. CFD predictions of the pressure inside and outside the enclosure and of the flame front shape are compared against experimental measurements. The comparison indicates a much better performance of the new approach compared to the initial model.

1.0 INTRODUCTION

Hydrogen use is expected to increase in the near future and its explosive nature brings up significant safety issues. In the case of an accident, hydrogen mixes with air and forms a flammable cloud. An accidental release in closed space can have catastrophic consequences in the case of an explosion. The confined space will lead to the development of much higher over-pressure compared to a similar explosion in open space. The venting of the hot products out of the closed space is the final protection measure in order to mitigate the damages of the explosion. Even though there are guidelines for the minimum size of the vent for a given space, these are not reliable and commonly accepted [1]. In the past years, the increase of computational power has rendered Computational Fluid Dynamics (CFD) as a very attractive methodology for risk assessment. With its high numerical accuracy, it can evaluate regulations and standards and give deeper insight into the physical phenomenon.

An experiment revealing the complexity of vented hydrogen explosions was carried out by Cooper et al. [2]. Four characteristic over-pressure peaks were identified: The first one took place because of the opening of the vent, the second one was caused by the external explosion, the third one by the reduction of the combustion rate when the flame touches the walls and the last one by the instabilities which enhance the combustion process due to flame-acoustic interaction. The magnitude of these peaks and the identification of the most dangerous ones depend on many factors, such as the geometry of the confined space, the vent size, the mixture composition and the ignition position.

External explosion is a phenomenon of increased importance in vented geometers because it can significantly increase the internal pressure. As the combustion develops inside the enclosure, unburned mixture is pushed outside through the vent. When the flame reaches the vent, this mixture starts burning creating a secondary explosion. This explosion seems to have much more strength than the internal one. The main reasons that have been proposed for that behavior are the creation of extensive turbulence in the area outside the vent because of the jet-like flow, and the development of Rayleigh-Taylor instability due to the acceleration of the less dense products through the vent to the more dense unburned mixture. Both reasons potentially lead to an augmentation of the reaction rate which leads to a violent external explosion. The pressure increase in the area outside the vent causes the decrease of the venting rate and consequently the increase of the internal pressure. A recent analysis of the peak over-pressures in vented explosion has been made by Chao et al. [3], where the effects of fuel, enclosure size, ignition location, vent size and obstacles were examined. Special attention to external explosion has been paid in several works such in [4], [5], [6] and [7].

CFD modeling of deflagrations is a big challenge. Combustion occurs at very small scales of the order of millimeters whereas geometries of practice interest are of order of meters. Turbulence plays a significant role and even the modeling of isothermal turbulent flow is subject of open research. The growth of instabilities at the flame front, the complex interaction between the flame and the turbulence along with the very wide range of applications, make the modeling a difficult task. As a result there is no model which is superior for all applications. External explosion introduce an addition difficulty in deflagration modelling. Molkov et al. [8] [9] performed Large Eddy Simulation (LES) to model a large-scale explosion in a vented enclosure (10 x 8.75 x 6.25 m), revealing the issue of external explosion modeling. In order to reproduce the experimental results, the combustion rate needed to be increased by approximately a factor of 2 at the area outside the vent. A similar approach was followed by Makarov et al. [10] in vented explosion through relief pipe. Bauwens et al. [11] and Keenan et al. [12] simulated hydrogen deflagrations in a vented room (4.6 x 4.6 x 3.0 m) focusing on the modeling of Rayleigh-Taylor instability for the correct reproduction of external explosion. The instability was modelled through an additional transport equation which takes into account the generation and the suppression rate of the instability.

In the current work, a hydrogen vented deflagration experiment is simulated using the CFD methodology. The primary objective is the accurate prediction of the external explosion phenomenon. A new approach is presented and is evaluated against the experiment.

2.0 EXPERIMENTAL DESCRIPTION

In order to evaluate the new modelling approach, a hydrogen deflagration experiment performed by KIT is chosen [13]. The experimental facility consists of an empty enclosure of 0.98 x 0.96 x 1.0 m (length x width x height) with a vent 0.5 x 0.5 m in size located in the center of a wall. Homogeneous 18% hydrogen-air mixture fills the enclosure. The mixture is ignited at the center of the opposite to the vent wall (back-wall ignition).

This experiment was chosen for the following reasons. Firstly, it is a reliable experiment and the data regarding its reproducibility are available. Secondly, there are many experimental data available. Pressure and temperature were measured at several locations both inside and outside the enclosure. Furthermore, visualization of the burned and the unburned mixture was made, using the BOS-schlieren technique. As a result the general shape of the flame front can be compared against the experiment. Finally, the study of the experimental data [13] reveled the violence of the external explosion phenomenon and the impact on the internal pressure which means that we can evaluate our model against this phenomenon.

3.0 NUMERICAL MODELLING

3.1 RMS turbulence velocity

The main issue in deflagration modeling is the estimation of the reaction rate. The combustion process occurs typically in a very thin area (flame front) which propagates in space. In real case scenarios, this area is very small compared to the length scale of the problem. Consequently, the flame front cannot be resolved and the turbulence-flame interactions need to be modelled. Turbulence is usually descripted through the Root-Mean-Square (RMS) turbulence velocity u_0'. In combustion modelling, the rms velocity almost always appears in the estimation of the reaction rate, in order to quantify turbulence and its influence to the combustion. This velocity is usually estimated through the turbulent kinetic energy k, assuming isotropic turbulence:

$$u_0' = \sqrt{2k/3} \tag{1}$$

In LES methodology the subgrid turbulent kinetic energy is usually used which is estimated based on the subgrid diffusivity μ_{sgs} from the relation

$$k_{sgs} = \frac{\mu_{sgs}^2}{\rho^2 L_{sgs}^2} \tag{2}$$

where L_{sgs} is the subgrid length scale, estimated through the relation $L_{sgs} = C_s \Delta$ in the classical Smagorinsky model where C_s is the Smagorinsky constant and Δ the filter size.

The problem of u_0' estimation was posed by Colin et al. [14]. A series of arguments is presented which question the validity of the above relations, especially in LES because of the dependency of μ_{sgs} on the strain rate in a Smagorinsky type subgrid model. The main argument is that this kind of models has been developed mainly for isothermal flows and as a result they are not suitable for combustion modelling because they may be affected by the thermal expansion. One of the consequences is the overestimation of the subgrid diffusivity and thus of the turbulent burning velocity in the case of low turbulence. The problem of u_0' estimation is also stated by Poinsot & Veynante [15]. They point out that in experiments u_0' is calculated in the unburned region whereas in most simulations u_0' is estimated inside the flame according to the local characteristics of the flow.

In order to deal with the above issues, Colin et al. [14] proposed a different relation. This relation estimates different rms turbulence velocity for each velocity component based on the Laplacian of the resolved vorticity field:

$$\vec{u}_0' = c\Delta^3 \left[\nabla^2 \left(\nabla \times \vec{u} \right) \right] = c\Delta^3 \left[\nabla \times \left(\nabla^2 (\vec{u}) \right) \right] \tag{3}$$

The ∇^2 operator is applied in each element of the $\nabla \times \vec{u}$ (in the first equality) or of the $\vec{u}$ (in the second equality) vector, in order to obtain the three component of the rms turbulence velocity. The constant c was estimated equal to 2 based on the Kolmogorov spectrum [14]. This method naturally subtracts the dilatational part of the velocity field. As a result the rms turbulence velocity remains zero in regions of irrotational volumetric expansion, such as in the case of a plane laminar flame. We should note that for the calculation of the second order derivatives, a step size of 2Δ is used in order to exclude the impact of the smallest scales which are not well resolved. For example, for equidistance grid the following relation is used:

$$\left. \frac{\partial^2 u}{\partial x^2} \right|_i = \frac{u_{i+2} - 2u_i + u_{i-2}}{\left(2\Delta x\right)^2} \tag{4}$$

where u a velocity component and i the cell index. More details can be found in [14]. This approach has also been used successfully by Charlette et al. in [16].

3.2 Governing equations - Combustion model

For the CFD simulations the ADREA_HF code was used [17]. The model used solves the space-averaged Navier-Stokes equations along with the energy equation (conservation equation of static enthalpy) and the conservation equation of each of the mass fraction of the species that take part in the combustion process. The multi-component mixture is assumed to be in thermodynamic equilibrium. The equation of state for ideal gases relates pressure with density and temperature. For turbulence, the RNG LES methodology was used. The set of the main equations that was used are presented in [18].

Combustion is modelled using the "Multi-phenomena turbulent burning velocity" model developed in Ulster University [19]. In this model, the turbulent burning velocity is calculated based on a modification of Yakhot's equation, in order to account for all the main physical mechanisms which appear in hydrogen deflagrations such as the turbulence generated by the flame front itself, preferential diffusion and fractal structure of the flame front:

$$S_t = \Xi_k \cdot \Xi_{lp} \cdot \Xi_f \cdot S_u \cdot \exp\left(\frac{u_0'}{S_t}\right)^2 \tag{5}$$

In this relation, S_t is the turbulent burning velocity, S_u the laminar burning velocity (function of pressure) and Ξ are factors that account for the various mechanisms which accelerate the combustion process. Details about the implementation in the ADREA_HF can be found in [18], [20]. The values of the main parameters that were used in the present simulations are:

$$\Xi_k^{\max} = 3.0\,,\ R_0 = 1.0\ m\,,\ \psi = 0.9\,,\ S_{u0} = 0.64\ m/s\,,\ \varepsilon = 0.66\,,\ \Xi_{lp} = 1.96 \tag{6}$$

where $\Xi_k^{\max}$ is the maximum value of the wrinkling factor Ξ_k (turbulence generated by the flame front), R_0 the critical radius where the turbulence is fully developed, ψ a model constant, S_{u0} the laminar burning velocity at initial conditions, ε the overall thermo-kinetic index and Ξ_{lp} the factor which accounts for the leading point concept. Due to the medium scale of the experiment, the fractal submodel is not crucial (Ξ_f values are close to one) and could be omitted without an impact on the results.

In the initial model, u_0' is estimated based on the equations (1) and (2). In this work, equation (3) is also used in order to evaluate it against the experiment. Charlette et al. [16], used equation (3) along with a different (instead of Yakhot's equation) relation for the turbulent burning velocity. In order to study the effect of the turbulent burning velocity equation, the relation of Charlette et al. is also tested. This relation is:

$$S_t = S_u'\left(1 + \min\left[\frac{\Delta}{\delta_l^0}, \Gamma\frac{u_0'}{S_u'}\right]\right)^{\beta} \tag{7}$$

where β is equal to 0.5, Δ the cell size and δ_l^0 the laminar flame thickness (equal to $0.370 \cdot 10^{-3}$ m in our case). Γ is a function of Δ/δ_l^0 and u_0'/S_u' (efficiency function) which was estimated from DNS results of flame-vortex interaction [16]. Equation (7) was developed specifically to be used in the frame of LES methodology. In the original model, S_u' is the unstrained laminar flame speed. However here, following the concepts of the "Multi-phenomena turbulent burning velocity", S_u' is set equal to the subgrid scale burning velocity, thus:

$$S_u' = \Xi_k \cdot \Xi_{lp} \cdot \Xi_f \cdot S_u \tag{8}$$

In Figure 1, the comparison of the turbulent burning velocity formula of Yakhot and of Charlette et al. is shown. We observe that for low turbulence (u_0'/S_u' approximately lower than 1), Yakhot's equation produces higher values of S_t compared to Charlette's formula. For more intense turbulence and values of Δ/δ_l^0 greater than 20, Yakhot's equation produces lower values of S_t. A significant different between the models is that Charlette's formula is consistent with the "bending effect" because for high turbulence S_t becomes independent of u_0'/S_u'. On the other hand in Yakhot's equation S_t continually

increases with increasing u_0'/S_u'. This means that eventually at very high values of u_0'/S_u' Yakhot's equation will give higher values of S_t compared to Charlette's formula. In our case, the value of Δ/δ_l^0 parameter is equal to 54 (approximately, green line in the diagram).

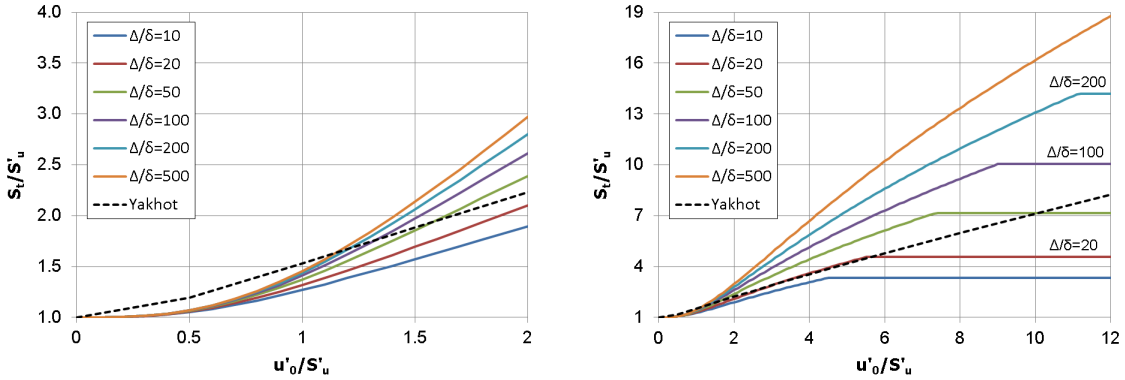

Figure 1. Comparison of the turbulent burning velocity of Yakhot's equation (black dashed line) and of Charlette et al. for different values of the parameter Δ/δ_l^0 (colored lines). Left: values of u_0'/S_u' from 0 to 2, Right: values of u_0'/S_u' from 0 to 12

3.3 Numerical details

ADREA-HF uses the finite volume method on a staggered Cartesian grid. Two grids were used in order to examine grid independency. The total number of cells in Grid 1 was 1,438,770 and in Grid 2 2,656,742. The resolution inside the chamber and at the area outside the vent (up to a distance of 0.85 m from the vent) is 0.020 m in Grid 1 and 0.015 m in Grid 2. The geometry, the domain and two planes of Grid 1 are shown in Figure 2. The enclosure is located inside a room, as in the experiment. The room is considered completed closed, although some small openings existed in the experiment.

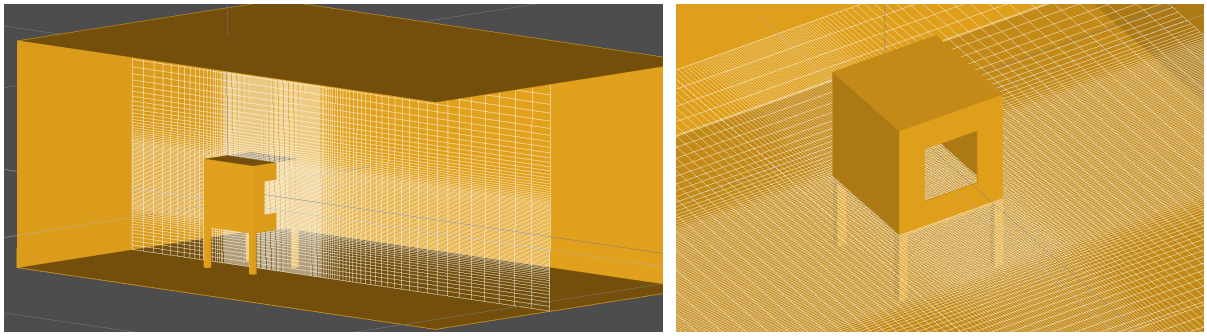

Figure 2. Geometry, domain and grid used in the simulations

The pressure and velocity equations are decoupled using a modification of the SIMPLER algorithm. For the discretization of the convective terms in the momentum equations a second order accurate bounded central scheme was used while in the conservation equations of species and energy a second order accurate bounded linear upwind scheme. The implementation was carried out using a deferred-correction approach via the source term. For the time advancement, the second order accurate Crank-Nicolson numerical scheme was chosen. The time step is automatically adapted according to prescribed error bands and the desired Courant–Friedrichs–Lewy (CFL) number. CFL maximum value was set equal to 0.1. As initial conditions, a stagnant flow field with no turbulence is specified. Ignition is modelled by fixing the reaction rate in a cell at the ignition point, in order the initial amount of fuel to be burned at a determined interval. This interval was set equal to 0.003 and 0.002 s for Grid 1 and Grid 2 respectively.

4.0 RESULTS AND DISCUSSION

In Figure 3 the pressure time series are presented inside and outside the enclosure for the experiment and the simulations. To begin with, simulation results are similar between Grid 1 and Grid 2. Thus, in the following analysis the results of Grid 1 are discussed. Furthermore, the rest of the simulations were conducted using this grid.

Experimental results reveal the effect of the external explosion. In Figure 4 (first row) the flame position in the experiment is shown at 0.086, 0.0893 and 0.091 s. We observe that at 0.086 s the flame passes through the vent. This is the time where the pressure inside the room stops increasing (Figure 3). An approximately constant overpressure value of 5.2 kPa is maintained until 0.092 s. At this time, the pressure inside the room is rapidly increased because of the external explosion. As we can see in Figure 3, the external pressure (which was measured at a distance of 0.24 m from the vent) is rapidly increased at approximately 0.09 s. This affects the internal pressure which is also rapidly increased until 0.097 s where the pressure peak occurs.

Simulation results are qualitatively similar to the experimental one until the occurrence of the main pressure peak. However, significant quantitative differences are observed. Firstly, the pressure is increased sooner than the experiment. However, similar to the experiment, the increase is stopped at the time when the flame passes the vent (0.078 s). This is shown in Figure 4 (second row) where the predicted flame front is shown along with the overpressure contour lines. The pressure remains approximately constant until 0.085 s (Figure 3). At this time, the pressure inside the enclosure is increased again, following the increase of the pressure outside the vent due to the external explosion. However, the rate of pressure rise both inside and outside the enclosure is much lower than the experiment, which leads to smaller maximum overpressures. The predicted maximum overpressures inside and outside the enclosure are equal to 6.9 kPa and 2.8 kPa respectively whereas the experimental values are equal to 10.3 kPa and 5.0 kPa. Comparing the flame front shapes between the experiment and the simulation (Figure 4), we observe some significant differences. In experiment, a spherical-like flame shape is formed. On the other hand in the simulation, the front spreads more in the horizontal direction and forms a mushroom-like shape. Then the tips of the mushroom-like shape are rolled-up by the vortices. From the above, it can be concluded that the simulation fails to reproduce the external explosion.

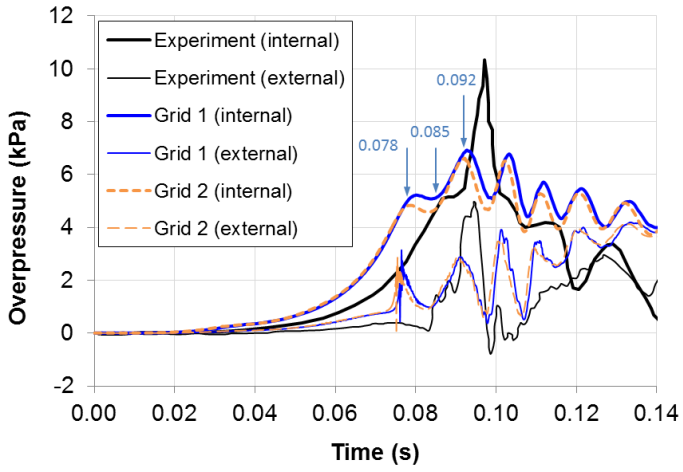

Figure 3. Internal and external (0.24 m from the vent) pressure time series for experiment and simulations. The arrows refer to the contours in Figure 4

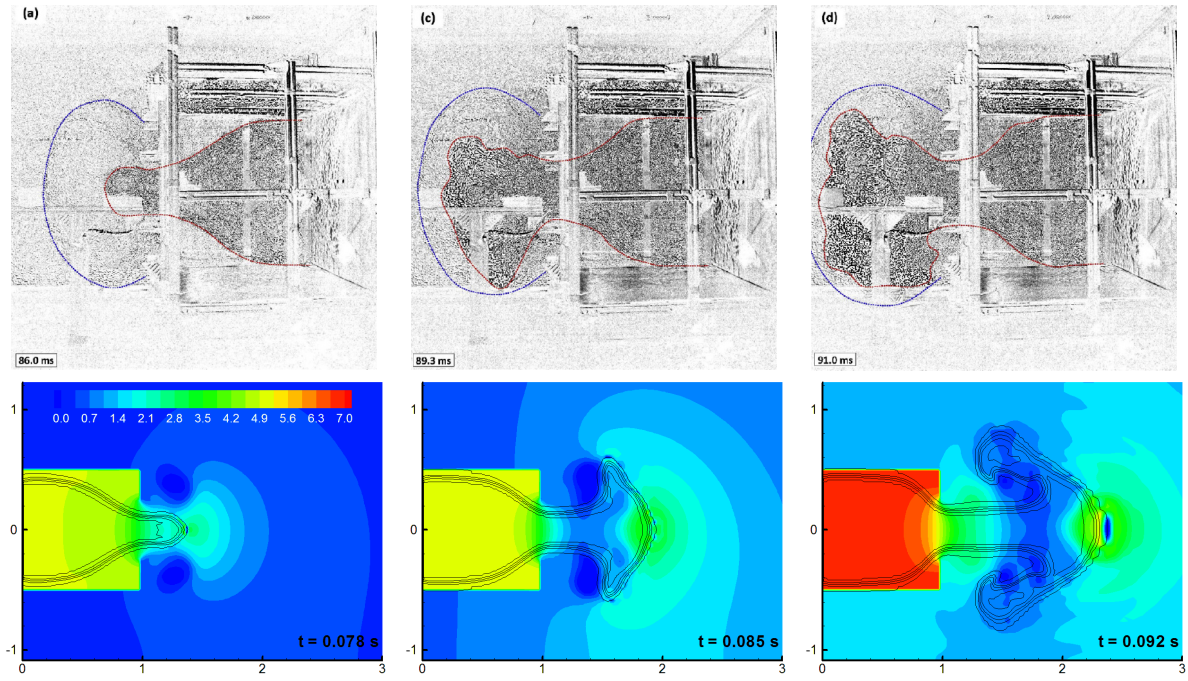

Figure 4. Flame front position in the experiment [13] (red line – top) and in the simulations in the central XZ plane (black lines – bottom). Overpressure contours (kPa) are also shown in simulation

In Figure 5 the main variables of the combustion model are presented as a function of time, averaged in the flame front. In the left diagram, the laminar flame speed S_u and the Ξ factors are shown. We observe that the factors that have the greatest contribution in flame acceleration are the Ξ_{lp} and the Ξ_k. The Ξ_{lp} factor obtains its maximum value in a short time because thermo-diffusion instability is developed quite fast. On the other hand, the Ξ_k factor which is related to the turbulence generated by the flame front itself, obtains its maximum value at the end of the explosion. Both factors increase the laminar flame speed up to 4 times. In the right diagram, S_t along with the rms velocity u_0' and the subgrid scale burning velocity S_u' are presented. We observe that until 0.078 s the S_t line is very close to the S_u' line due to the low values of u_0'. After that time, the flame exits the enclosure and the average u_0' increases because of the high turbulence region outside the vent. As a result, S_t also increases too, deviating from the S_u' line. This increase, however, is small and it is not able to reproduce the violence of the external explosion.

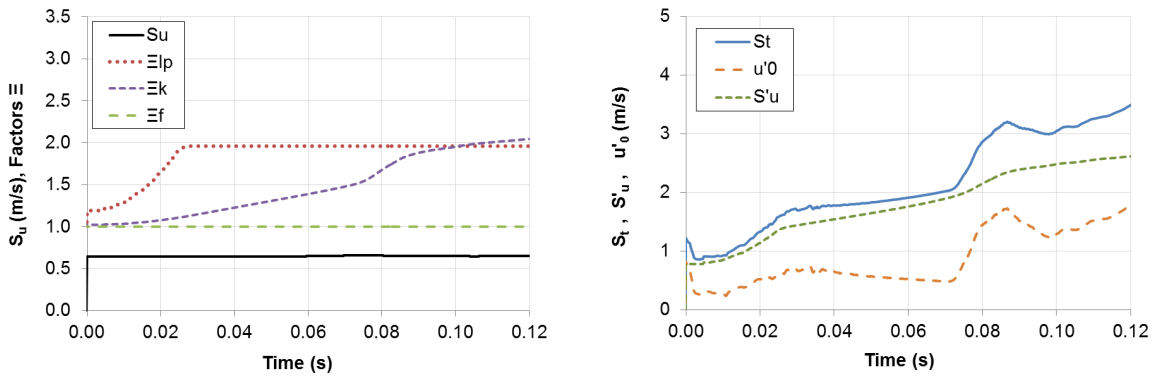

Figure 5. Laminar flame speed S_u along with Ξ factors (left) and turbulent burning velocity S_t along with the rms velocity u_0' and the subgrid scale burning velocity S_u' (right) as a function of time. Mean values in the flame front

In Figure 6, the comparison of the pressure time series between the initial and the modified combustion models are presented. “Initial model” refers to the original “Multi-phenomena turbulent burning velocity”, “Model 1” refers to the modification in the rms turbulence velocity calculation and “Model 2” refers to the modification in both the rms velocity and the turbulent burning velocity (Charlette’s formula instead of Yakhot’s formula – Section 3.2).

We observe that the results of Model 1 and Model 2 are similar and in better agreement with the experiment compared to the initial model. The new models are able to predict the rapid increase of the external pressure which leads to the increase of the internal one. The maximum overpressure inside and outside the enclosure is predicted satisfactory by both models. Comparing the overpressure inside the facility between Model 1 and initial model (Figure 6, left), we observe that the curves are almost identical until the time when the flame front exits the enclosure. After that time, the pressure continues to increase in Model 1 reaching the value of 9.4 kPa at 0.09 s. Comparing Model 1 with Model 2 (Figure 6, right) the only difference is a small time-delay that is observed in Model 2. This delay makes the overpressure curve to be in much better agreement with the experiment until the time of approximately 0.078 s.

The flame position is shown in Figure 7 for the Model 2 case. We observe that the shape of the flame front outside the vent has a spherical-like form which is much closer to the experiment than the initial model (Figure 4).

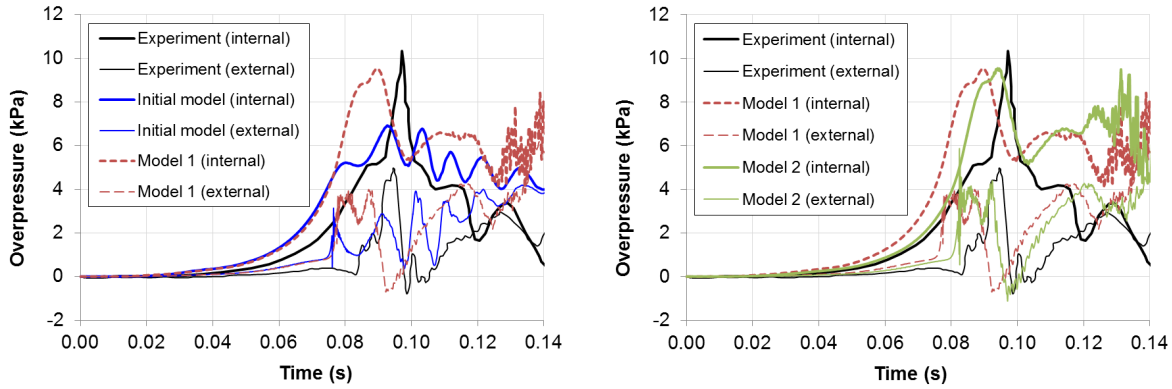

Figure 6. Internal and external (0.24 m from the vent) pressure time series for experiment and simulations. Model 1 and Model 2 refer to the new formula for the rms turbulence velocity along with the Yakhot’s and Charlette’s equation respectively

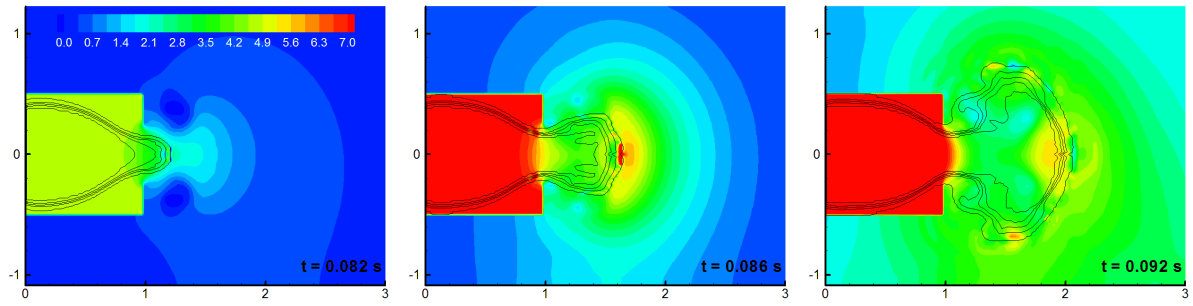

Figure 7. Flame front position (black lines) along with the overpressure contours (kPa) in the central XZ plane for Model 2 case

The differences between the modified combustion models and the initial one are explained by the values of the rms turbulence velocity that the models predict. In Figure 8, the average values of the turbulent burning velocity S_t and the rms velocity u_0' are presented as a function of time for the initial

and the modified models. We observe that until the time of 0.076 s (time at which the flame reaches the vent) all models predict very similar values of u_0'. As a result Model 1 predicts the same overpressure values with the initial model, as we saw in Figure 6. On the other hand, the small time-delay of the overpressure curve that is observed in Model 2 (Figure 6), is attributed to the smaller turbulent burning velocity that Charlette's formula predicts compared to Yakhot's equation at low values of u_0'/S_u' (Figure 1). The values of the rms turbulence velocities are low at the initial stages of combustion and thus this difference is emerged. After 0.076 s, we observe that the rms velocity increases rapidly in both Model 1 and Model 2 cases. The values of u_0' are much higher than the values predicted from the initial model. Consequently, turbulent burning velocity S_t is higher too resulting in higher overpressures.

The high values of u_0' in the new models are predicted in the area outside the vent where large eddies are formed. This can be seen in Figure 9 (top), where the contours of u_0' are presented along with the flame front. This behavior is in accordance with the physics of the phenomenon because high turbulence is expected to be developed in the area where high values of u_0' are predicted by the model. In the same figure, the contours of u_0' are presented for the initial model. The shape of the contours is similar between models. However, much smaller values are predicted in the initial model.

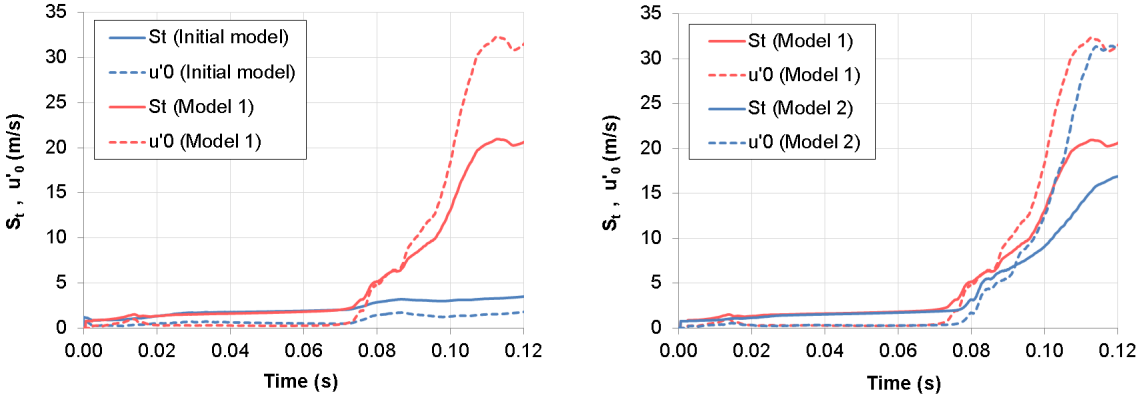

Figure 8. Turbulent burning velocity S_t and rms velocity u_0' as a function of time for the initial and the modified models. Mean values in the flame front

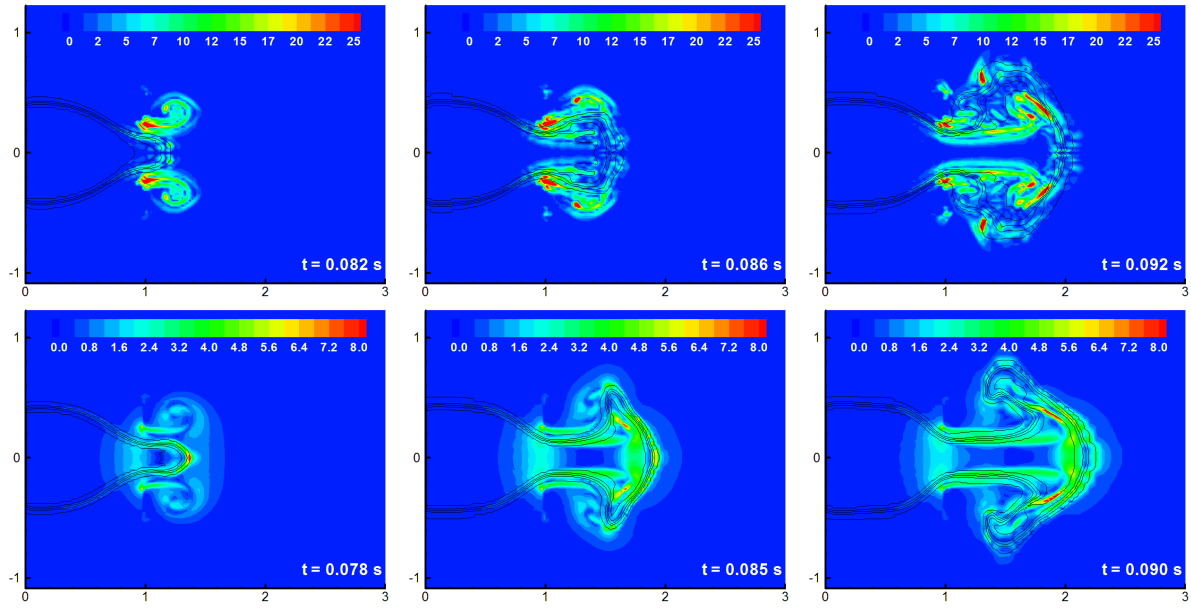

Figure 9. RMS turbulence velocity (m/s) along with the flame front position in the central XZ plane for Model 2 (top) and Initial model (bottom) case

5.0 CONCLUSIONS

A new CFD model for vented deflagration simulations was presented. This model faces the problem of the correct prediction of the external explosion phenomenon which usually occurs in vented deflagrations. The main characteristic of the new model is the way that the rms turbulence velocity is estimated. This velocity is calculated based on the Laplacian of the resolved vorticity field and not using the usual approach of the subgrid diffusivity. This is an attractive approach in Large Eddy Simulation because the impact of the resolved eddies on the unresolved flame front are taken into account. The new model was successfully validated against a medium-scale vented deflagration experiment. The sudden increase of the external pressure and the influence on the internal pressure was well predicted in contrast to the original model which failed to predict the overpressure peak. Another formula for the turbulent burning velocity instead of Yakhot's equation was also tested. The new formula exhibited similar behavior. The only difference was a small time-delay in the pressure curve which can be explained by the form of the equations.

ACKNOWLEDGEMENTS

This work was funded by NCSR Demokritos and the private sector in the framework of the research program "Establishing a Multidisciplianary and Effective Innovation and Entrepreneurship Hub". The authors would also like to acknowledge the project HyIndoor (Grant agreement no: 278534) for the access in the experimental data.

REFERENCES

1. Bauwens, C.R. and Dorofeev, S.B., Effect of initial turbulence on vented explosion overpressures from lean hydrogen–air deflagrations, *Int. J. Hydrogen Energy*, **39**, No. 35, 2014, pp. 20509–20515.
2. Cooper, M.G., Fairweather, M. and Tite, J.P., On the mechanisms of pressure generation in vented explosions, *Combust. Flame*, **65**, No. 1, 1986, pp. 1–14.
3. Chao, J., Bauwens, C.R. and Dorofeev, S.B., An analysis of peak overpressures in vented gaseous explosions, *Proc. Combust. Inst.*, **33**, No. 2, 2011, pp. 2367–2374.
4. Harrison, A.J. and Eyre, J.A., External Explosions as a Result of Explosion Venting, *Combust. Sci. Technol.*, **52**, No. 1–3, 1987, pp. 91–106.
5. Jiang, X., Fan, B., Ye, J. and Dong, G., Experimental investigations on the external pressure during venting, *J. Loss Prev. Process Ind.*, **18**, No. 1, 2005, pp. 21–26.
6. Ferrara, G., Willacy, S.K., Phylaktou, H.N., Andrews, G.E., Di Benedetto, A., Salzano, E. and Russo, G., Venting of gas explosion through relief ducts: Interaction between internal and external explosions, *J. Hazard. Mater.*, **155**, No. 1, 2008, pp. 358–368.
7. Proust, C. and Leprette, E., The dynamics of vented gas explosions, *Process Saf. Prog.*, **29**, No. 3, 2009, pp. 231–235.
8. Molkov, V.V. and Makarov, D.V., Rethinking the Physics of a Large-Scale Vented Explosion and its Mitigation, *Process Saf. Environ. Prot.*, **84**, No. 1, 2006, pp. 33–39.
9. Molkov, V., Makarov, D. and Puttock, J., The nature and large eddy simulation of coherent deflagrations in a vented enclosure-atmosphere system, *J. Loss Prev. Process Ind.*, **19**, 2006, No. 2–3, pp. 121–129.
10. Makarov, D., Verbecke, F. and Molkov, V., Numerical analysis of hydrogen deflagration mitigation by venting through a duct, *J. Loss Prev. Process Ind.*, **20**, No. 4–6, 2007, pp. 433–438.
11. Bauwens, C.R., Chaffee, J. and Dorofeev, S.B., Vented explosion overpressures from combustion of hydrogen and hydrocarbon mixtures, *Int. J. Hydrogen Energy*, **36**, No. 3, 2011, pp. 2329–2336.

12. Keenan, J.J., Makarov, D.V. and Molkov, V.V., Rayleigh–Taylor instability: Modelling and effect on coherent deflagrations, *Int. J. Hydrogen Energy*, **39**, No. 35, 2014, pp. 20467–20473.
13. Kuznetsov, M., Friedrich, A., Stern, G., Kotchourko, N., Jallais, S. and L'Hostis, B., Medium-scale experiments on vented hydrogen deflagration, *J. Loss Prev. Process Ind.*, **36**, 2015, pp. 416–428.
14. Colin, O., Ducros, F., Veynante, D. and Poinsot, T., A thickened flame model for large eddy simulations of turbulent premixed combustion, *Phys. Fluids*, **12**, No. 7, 2000, pp. 1843–1863.
15. Poinsot, T. and Veynante, D., Theoretical and Numerical Combustion, Second Edition, 2005, R.T. Edwards, Inc.; 2nd edition.
16. Charlette, F., Meneveau, C. and Veynante, D., A power-law flame wrinkling model for LES of premixed turbulent combustion Part I: non-dynamic formulation and initial tests, *Combust. Flame*, **131**, No. 1–2, 2002, pp. 159–180.
17. Venetsanos, A.G., Papanikolaou, E.A. and Bartzis, J.G., The ADREA-HF CFD code for consequence assessment of hydrogen applications, *Int. J. Hydrogen Energy*, **35**, No. 8, 2010, pp. 3908–3918.
18. Tolias, I.C., Venetsanos, A.G., Markatos, N. and Kiranoudis, C.T., CFD modeling of hydrogen deflagration in a tunnel, *Int. J. Hydrogen Energy*, **39**, No. 35, 2014, pp. 20538–20546.
19. Molkov, V.V., Fundamentals of hydrogen safety engineering, 2012, www.bookboon.com.
20. Tolias, I.C., Venetsanos, A.G., Markatos, N. and Kiranoudis, C.T., CFD evaluation against a large scale unconfined hydrogen deflagration, *Int. J. Hydrogen Energy*, 2016, in press.